ORGANOMETALLICS

pubs.acs.org/Organometallics Article

Modifying Phosphorus(III) Substituents to Activate Remote Ligand-Centered Reactivity in Triaminoborane Ligands

Kyounghoon Lee, Johnathan D. Culpepper, Riffat Parveen, Dale C. Swenson, Bess Vlaisavljevich,* and Scott R. Daly*

Cite This: *Organometallics* 2020, 39, 2526−2533 Read Online

ACCESS | Metrics & More | Article Recommendations | Supporting Information

ABSTRACT: Triaminoborane-bridged diphosphorus ligands called TBDPhos can undergo cooperative ligand-centered reactions at the 1,8,10,9-triazaboradecalin (TBD) backbone while bound to metals, but the factors that control this reactivity are not well understood. Previous studies showed that TBDPhos reactivity is highly sensitive to phosphorus substituents, ancillary ligands, and metal coordination environment despite these changes being significantly removed from the reactive N−B bond. Here we describe how exchanging phenyl and ethyl substituents attached to phosphorus with methoxy turns on ligand-centered reactions in otherwise unreactive (TBDPhos)Pt($S_2C_6H_4$) and (TBDPhos)-Mo$(CO)_4$ complexes. The synthesis and characterization of the complexes are described alongside comparative reactivity studies using MeOH as a simple but effective test substrate. Complementary density functional theory (DFT) calculations on an expanded series of (TBDPhos)Pt($S_2C_6H_4$) complexes corroborate the experimental results and show that both size and electronic properties of the phosphorus substituents can significantly influence the Gibbs free energy of reaction at the remote ligand site. These results demonstrate how seemingly ancillary ligand modifications can levy significant control over ligand-centered reactivity in TBDPhos complexes, which may be relevant when considering the design of other chemically reactive ligands with Lewis acidic functional groups.

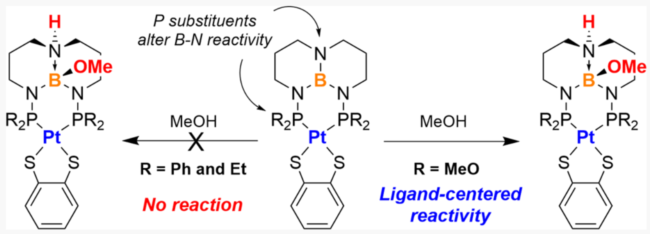

■ INTRODUCTION

Incorporating Lewis acids into ligands has proven to be a fruitful strategy for accessing new types of reactivity with transition metal complexes.[1−14] Borane-containing ligands have been used to assist metals in stoichiometric reactions,[15−21] substrate capture and activation,[22−32] and catalysis.[33−43] The primary design considerations when preparing reactive borane ligands are often Lewis acid strength as dictated by the substituents attached to boron and the proximity and orientation of the reactive site with respect to the metal (e.g., inner vs outer sphere). In contrast, it is less often considered how ligand modifications further removed from the borane may influence reactivity.

Recently, our group reported a new class of diphosphorus ligands called TBDPhos (Scheme 1).[44] These ligands contain a bicyclic triaminoborane called 1,8,10,9-triazaboradecalin (TBD)[45,46] that can undergo cooperative ligand-centered reactions when bound to metals. Treating (^{Ph}TBDPhos)MCl_2 complexes (where M = Ni or Pd) with Brønsted acids and hydrated fluoride salts, for example, yielded net *trans* addition of H−X (X = OH, OR, Cl, and F) across the bridgehead N−B bond (Scheme 1).[44,47] These reactions are referred to as cooperative because protonation of the bridgehead nitrogen appears to be a prerequisite for accessing reactivity at the borane.[44]

Scheme 1. Comparison of Ligand-Centered Reactions with Different TBDPhos Complexes and MeOH

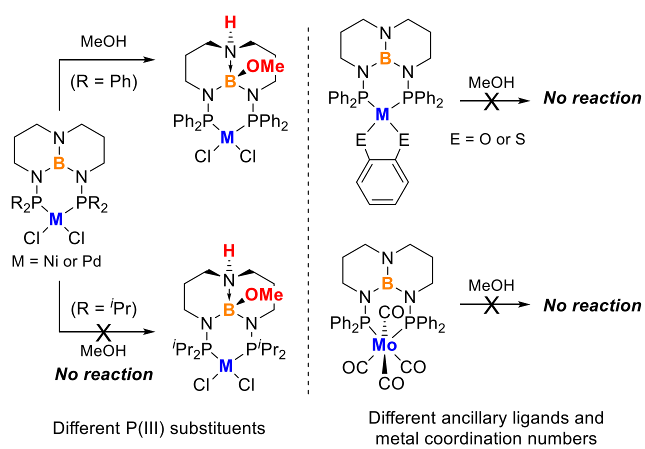

Received: May 11, 2020
Published: June 25, 2020

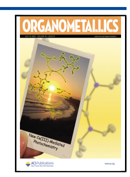

During our initial investigation of TBDPhos complexes, we discovered that ligand-centered reactivity can be significantly diminished by exchanging phosphorus substituents or altering the metal coordination environment, despite these modifications being significantly removed from the TBD backbone. For example, we have shown that TBDPhos reactivity is attenuated by replacing phenyl substituents in square planar (^{Ph}TBDPhos)NiCl$_2$ with isopropyl substituents or by substituting the ancillary chlorides with chelating S and O ligands (Scheme 1).[44,47] Furthermore, complexes such as octahedral (^{Ph}TBDPhos)Mo(CO)$_4$ show no obvious reactivity in the presence of water or alcohols.[48]

Our desire to use ligand centered TBDPhos reactivity for more practical applications requires a fundamental understanding as to how ligand modifications affect reactivity at the TBD backbone. We initially postulated that the observed reactivity differences with ^{Ph}TBDPhos and ^{iPr}TBDPhos complexes could be attributed in part to increased sterics around the metal, but questions remained about the electronic influence of these substituents. Attempts to quantify substituent-induced changes in the Lewis acidity of TBDPhos complexes using spectroscopic approaches such as the Gutmann–Beckett method[49−51] have so far been unsuccessful.[44] The cooperative nature of ligand-centered reactivity in TBDPhos complexes complicates Lewis acidity measurements at boron because nitrogen protonation appears to be required for reactions to proceed.

To overcome these issues so that electronic and steric contributions of phosphorus substituents to TBDPhos reactivity could be distinguished, we set out to screen the reactivity of different TBDPhos complexes under identical conditions using MeOH as a simple test substrate. MeOH was selected for this purpose because it serves as both solvent and substrate, which allowed us to avoid comparing reactions under different conditions in different solvents. In this report, we describe the synthesis of methoxy- and ethyl-substituted TBDPhos ligands for side-by-side comparisons with other known TBDPhos ligands. Methoxy and ethyl were selected because they have nearly identical steric profiles but different electronic properties. We show how electronic factors associated with the phosphorus substituents in ^{MeO}TBDPhos and ^{Et}TBDPhos indeed control cooperative ligand-centered reactivity at the triaminoborane backbone when compared in side-by-side studies with Pt and Mo complexes containing ^{Ph}TBDPhos. We also quantify the role that steric contributions have on TBDPhos reactivity using density functional theory (DFT) calculations in an extended analysis of structurally similar (TBDPhos)Pt(S$_2$C$_6$H$_4$) complexes.

■ RESULTS AND DISCUSSION

^{MeO}TBDPhos and ^{Et}TBDPhos were synthesized as described for ^{Ph}TBDPhos by treating TBD with 2 equiv of ClP(OMe)$_2$ or ClPEt$_2$ in the presence of NEt$_3$ in CH$_2$Cl$_2$. Multinuclear NMR spectroscopy, elemental analysis (EA), and/or electron ionization mass spectrometry (EI-MS) confirmed their formation. The ^{11}B NMR resonances for ^{MeO}TBDPhos (δ 24.7 ppm) and ^{Et}TBDPhos (δ 25.9 ppm) showed only slight variations compared to those for TBD and ^{Ph}TBDPhos at δ 22.4 ppm and δ 26.2 ppm, respectively. As expected for the phosphoramidite ligand, the ^{31}P NMR resonance for ^{MeO}TBDPhos was much more deshielded at δ 145.6 ppm compared to ^{Et}TBDPhos and ^{Ph}TBDPhos at δ 43.3 and 47.7 ppm, respectively.

(^{Ph}TBDPhos)PtCl$_2$ (**1**), (^{MeO}TBDPhos)PtCl$_2$ (**2**), and (^{Et}TBDPhos)PtCl$_2$ (**3**) were prepared by treating (COD)PtCl$_2$ with the corresponding diphosphorus ligand in CH$_2$Cl$_2$. Once isolated, **1**−**3** were converted to the dithiolate complexes (^{Ph}TBDPhos)Pt(S$_2$C$_6$H$_4$) (**4**), (^{MeO}TBDPhos)Pt(S$_2$C$_6$H$_4$) (**5**), and (^{Et}TBDPhos)Pt(S$_2$C$_6$H$_4$) (**6**) by addition of 1,2-benzenedithiol in the presence of excess NEt$_3$ (Scheme 2).

Scheme 2. Synthesis of Pt Complexes and Their Reactivity with MeOH

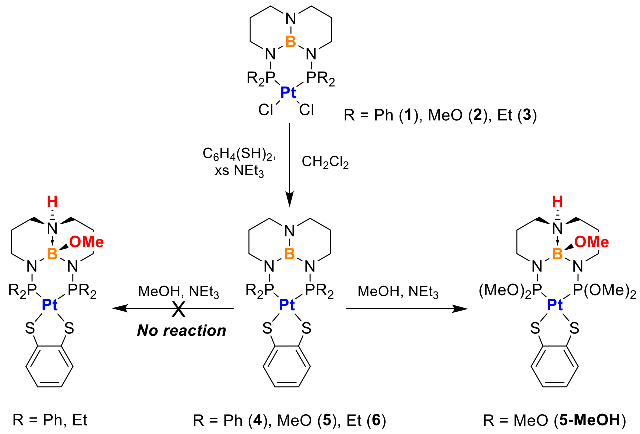

Crystals of **1**, **2**, **5**, and **6** were grown by vapor diffusion of Et$_2$O into CH$_2$Cl$_2$ solutions and XRD studies confirmed their square planar structures (Figures S1−S3). The bond distances and angles are similar to those observed for other Pt(II) diphosphorus complexes with chloride and 1,2-benzenedithiolate ligands (Table 1).[52−54] As is typical of TBDPhos complexes, the triaminoborane is rigorously trigonal planar, as indicated by the 360° sum of N−B−N angles. The bridgehead N−B bond distance in all of the complexes is 0.04−0.05 Å shorter than the two N−B bonds containing N atoms bound to P. The increased N−B double-bond character at the bridgehead position is consistent with its preferential reactivity over the other N−B bonds in ligand centered-reactions (vide infra).

NMR data collected for **1**−**6** were consistent with their formulations. The ^{11}B NMR spectra all revealed broad singlets that were shifted upfield ca. 1−2 ppm relative to their free ligands (Table 2). Not surprisingly, the ^{31}P NMR spectra revealed more pronounced differences, each showing diagnostic satellite peaks corresponding to ^{195}Pt−^{31}P coupling. $^{1}J_{PtP}$ coupling constants are known to correlate to Pt−P bond distance,[55] and the increase from 3730 Hz in **1** to 4895 Hz in **2** is consistent with the 0.02 Å decrease in Pt−P bond distances for **2** with ^{MeO}TBDPhos compared to **1**. The Pt−P bond distances of 2.206(2) and 2.218(2) Å in **5** are 0.02−0.03 Å longer than those for **2** due to the greater *trans* influence of the dithiolate ligand. The change in bond distance again corresponds to a decrease in the $^{1}J_{PtP}$ coupling constant from 4895 Hz in **2** to 3918 Hz in **5**.

We focused our reactivity studies on the dithiolate complexes **4**−**6**. These complexes were targeted to avoid complications associated with chloride lability and ligand exchange, as observed previously with (^{Ph}TBDPhos)NiCl$_2$ and (^{Ph}TBDPhos)PdCl$_2$,[44,47] because we are less confident about

Table 1. Selected Bond Distances (Å) and Angles (deg) from Single-Crystal XRD Data

	1	2	5	5-MeOH	6	7[a]	8	8-MeOH
M–P	2.2082(8)	2.1925(6)	2.206(2)	2.231(6)	2.246(3)	2.4887(7)	2.4392(5)	2.4409(5)
	2.2153(8)		2.218(2)	2.232(4)	2.235(3)	2.4946(8)	2.4428(5)	2.4564(5)
B–N	1.401(4)	1.409(5)	1.410(9)	1.65(1)	1.411(1)	1.415(4)	1.417(2)	1.668(2)
B–N(P)	1.453(4)	1.457(3)	1.451(9)	1.519(9)	1.457(2)	1.462(4)	1.465(2)	1.535(3)
	1.457(4)		1.459(8)	1.533(9)	1.455(1)	1.471(4)	1.468(2)	1.535(3)
P–N	1.657(3)	1.649(2)	1.654(5)	1.620(7)	1.681(7)	1.690(2)	1.660(2)	1.642(2)
	1.669(3)		1.647(5)	1.610(9)	1.676(4)	1.704(2)	1.667(1)	1.649(2)
B–O	–	–	–	1.441(8)	–	–	–	1.448(2)
M–L (eq)	2.3543(9)	2.3573(6)	2.317(2)	2.321(2)	2.323(5)	2.002(3)	2.009(2)	2.017(2)
	2.3631(8)		2.320(2)	2.326(2)	2.328(8)	2.007(3)	2.013(2)	2.019(2)
M–L (ax)	–	–	–	–	–	2.026(3)	2.037(2)	2.024(2)
	–	–	–	–	–	2.040(3)	2.039(2)	2.046(2)
P–M–P	92.20(3)	97.47(3)	94.04(6)	93.9(2)	95.58(5)	81.46(2)	88.13(2)	87.20(2)
ΣNBN	359.9(3)	360.0(2)	359.9(6)	328.3(6)	359.9(9)	359.7(2)	360.0(2)	330.2(1)

[a]Reported in ref 48.

Table 2. ^{11}B and ^{31}P NMR Resonances and M–P Coupling Constants (M = Mo and Pt) in $CDCl_3$[a]

compound	^{11}B	^{31}P{^{1}H}	$^1J_{MP}$ (Hz)[e]
^{Ph}TBDPhos[b]	26.2	47.7	–
^{MeO}TBDPhos	24.7	145.6	–
^{Et}TBDPhos	25.9	43.3	–
1	24.4	43.9	3730
2	22.7	69.9	4895
3	24.1	58.9	3692
4	24.9	53.3	2917
5	23.2	97.7	3918
5-MeOH[d]	1.7	97.3	3954
6	24.2	61.2	2912
7[c]	25.9	90.6	–
8	24.2	165.4	194
8-HNTf$_2$	27.8	167.0	–
8-MeOH[d]	2.7	165.3	192

[a]Chemical shifts are reported in δ units relative to $BF_3{\cdot}Et_2O$ (^{11}B) and 85% H_3PO_4 (^{31}P). [b]Ref 44. [c]Ref 48. [d]NEt_3 was added to the NMR sample. [e]No ^{95}Mo–^{31}P coupling was observed for **7** and **8-HNTf$_2$**.

the identity of the species that undergoes ligand-centered reactions in solution compared to the dithiolates. Incidentally, (^{Ph}TBDPhos)$PtCl_2$ (**1**) undergoes ligand-centered reactions with water and MeOH like its lighter congeners with Ni and Pd, as does the methoxy-substituted **2**, as told by the tell-tale ^{11}B NMR shifts indicating the change from three- to four-coordinate boron. Remarkably, ethyl-substituted **3** was completely unreactive with water or MeOH when tested under the same conditions.

The ligand-centered reactivities of **4**–**6** were tested by dissolving them in MeOH in the presence of a small amount of NEt_3, an additive that has been shown to enhance ligand-centered reaction rates with alcohols and water.[44,47] Our hypothesis is that NEt_3 helps to overcome the sluggish kinetics of these reactions by serving as a proton shuttle to facilitate *trans* addition of ROH to the TBD backbone. As reported previously for (^{Ph}TBDPhos)Ni($S_2C_6H_4$),[47] phenyl-substituted **4** showed no evidence of MeOH addition to the TBD backbone after mixing for 24 h, nor did ethyl-substituted **6**. In contrast, **5** immediately reacted with MeOH to form (^{MeO}TBDPhos-MeOH)Pt($S_2C_6H_4$) (**5-MeOH**), as indicated by the characteristic four-coordinate ^{11}B shift of δ 1.7 ppm. For comparison, *trans* addition of MeOH across the bridgehead N–B bond in (^{Ph}TBDPhos-MeOH)$NiCl_2$ and (^{Ph}TBDPhos-MeOH)$PdCl_2$ yielded ^{11}B NMR resonances of δ 1.9 and 3.2 ppm, respectively.[44] The ^{1}H NMR spectrum of **5-MeOH** also confirmed the addition of MeOH; two sets of diastereotopic resonances associated with the methoxy and propylene hydrogen atoms were observed due to loss of the mirror plane defined by the TBD backbone in **5**.

X-ray diffraction studies confirmed the formation of **5-MeOH** (Figure 1). The boron geometry is tetrahedral and the

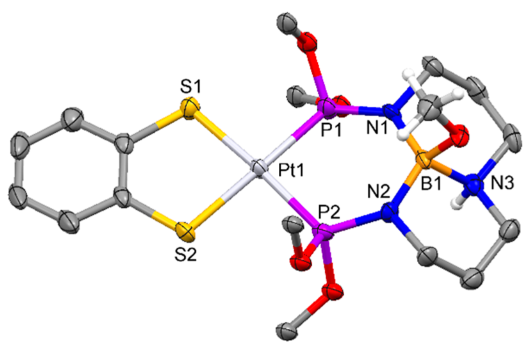

Figure 1. Molecular structure of **5-MeOH** with thermal ellipsoids at 50% level. Disordered fragments and hydrogen atoms not associated with added MeOH were omitted from the figure.

bridgehead N–B bond is formally a dative bond, as indicated by its 1.65(1) Å bond distance compared to 1.410(9) Å in the parent complex **5**. The remaining two N–B bonds lose their multiple bond character and increase from 1.451(9) and 1.459(8) Å in **5** to 1.519(9) and 1.533(9) Å in **5-MeOH**. The B–OMe bond distance of 1.441(8) Å is identical within error to the same bond in methanol-bound (^{Ph}TBDPhos-MeOH)-$NiCl_2$.[44]

Synthesis and Reactivity of Mo Complexes. As mentioned in the introduction, octahedral (^{Ph}TBDPhos)Mo-$(CO)_4$ (**7**) does not undergo reactions with MeOH, so we investigated if this reactivity changed with ^{MeO}TBDPhos.[48] No attempt was made to prepare the ^{Et}TBDPhos complex with Mo given that the Pt complex **6** showed no evidence of reactivity with this ligand.

(^{MeO}TBDPhos)Mo$(CO)_4$ (**8**) was prepared by refluxing a 1-to-1 mixture of $Mo(CO)_6$ and ^{MeO}TBDPhos in THF

https://dx.doi.org/10.1021/acs.organomet.0c00321
Organometallics 2020, 39, 2526–2533

overnight. NMR analysis of single crystals grown from Et_2O/pentane solutions revealed only a subtle shift in the ^{11}B NMR resonance compared to free ^{MeO}TBDPhos, but a new upfield ^{31}P NMR resonance assigned to **8** was observed at δ 165.4 ppm. In addition, the ^{31}P NMR spectrum confirmed metalation by revealing a sextet of satellites ($^1J_{MoP}$ = 194 Hz) with smaller intensity due to ^{31}P coupling with ^{95}Mo (I = 5/2; 15.9%). Single-crystal XRD studies confirmed the structure of **8** (Figure S4) and revealed subtle differences in the structural metrics when compared to **7** (Table 1). The Mo−P and P−N distances decreased by 0.03−0.04 Å in **8**, and the P−Mo−P bite angle increased from 82(1)° (**7**) to 88.13(2)° (**8**).

We tested the ligand-centered reactivity of **8** by dissolving it in MeOH in the presence of NEt_3, as described for **5** (Scheme 3). ^{11}B NMR analysis of the reaction mixture revealed the slow

Scheme 3. Synthesis and Reactivity Studies with Mo Complexes

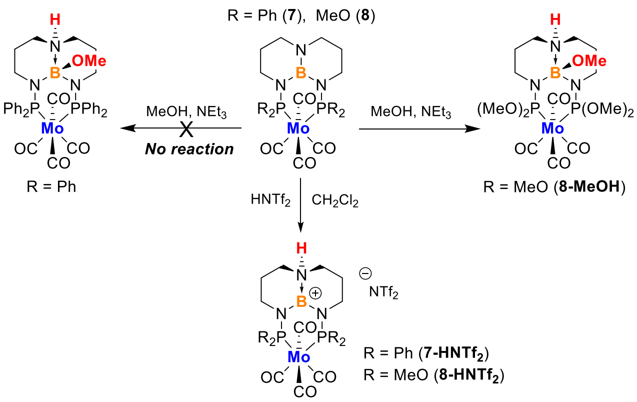

appearance of a new feature at δ 2.7, consistent with the transformation of three- to four-coordinate boron. XRD studies on single crystals grown by slow evaporation confirmed *trans* addition of MeOH across the TBD backbone in **8** to yield (^{MeO}TBDPhos-MeOH)$Mo(CO)_4$ (**8-MeOH**; Figure 2).

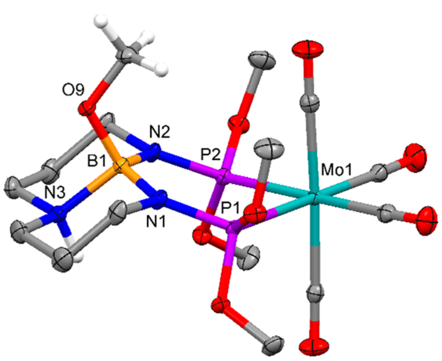

Figure 2. Molecular structure of **8-MeOH**. Ellipsoids are drawn at 50% probability. Hydrogen atoms not associated with added MeOH were omitted from the figure.

The characteristic trigonal planar to tetrahedral geometry change was again observed at boron along with characteristic elongation of all three B−N bonds. The B−OMe bond distances in **5-MeOH** and **8-MeOH** are identical despite the differences in metal and coordination environment.

We previously showed that treating **7** with strong Brønsted acids such as HOTf and $HNTf_2$ resulted in protonation of the bridgehead TBD nitrogen without chemically engaging the borane to yield the first structurally characterized examples of borenium ions (three-coordinate boron cations)[56−58] with TBDPhos.[48] We report here that this reactivity is also possible with ^{MeO}TBDPhos in **8** despite the increase in reactivity at boron. Treating **8** with $HNTf_2$ yielded a new complex with ^{11}B and ^{31}P NMR resonances shifted downfield to δ 27.8 and 167.0 ppm, respectively, compared to δ 24.2 and 165.4 ppm in **8**. The downfield ^{11}B shift is characteristic of formation of borenium ions due to the increased positive charge on boron. Although not structurally characterized like **7-HNTf$_2$**,[48] protonation of the bridgehead nitrogen on the TBD backbone was confirmed by IR and ^1H NMR spectroscopy. IR data collected on the solid revealed the N−H stretch at 3116 cm^{-1} and ^1H NMR data revealed the broadened N−H proton at δ 7.08 ppm.

IR data collected for **8**, **8-HNTf$_2$**, and **8-MeOH** revealed how ligand-centered reactions affect Mo-CO stretching frequencies (Table 3). Group theory predicts four IR active

Table 3. CO Stretching Frequencies and Assignments for Mo Complexes

compound	CO stretches (cm^{-1})	reference
7	2017, 1929, 1915, 1884	48
7-HNTf$_2$	2026, 1931, 1905	48
8	2025, 1924, 1903, 1889	this work
8-HNTf$_2$	2042, 1947, 1915	this work
8-MeOH	2018, 1933, 1909, 1872	this work

CO stretching bands for *cis*-$L_2M(CO)_4$ complexes in C_{2v} point group symmetry ($2A_1 + B_1 + B_2$), the highest energy and most resolved band being assigned to the symmetric A_1 stretch involving the axial CO ligands.[59] The A_1 stretching band for **8** was observed at 2025 cm^{-1} while the same stretch for **7** was observed at 2017 cm^{-1} (Figure 3). The 8 cm^{-1} increase for methoxy-substituted **8** relative to phenyl-substituted **7** is nearly identical to the 10 cm^{-1} increase reported previously for the same feature in the IR spectra of $[R_2P(CH_2)_2PR_2)]Mo(CO)_4$ when R = Ph (2023 cm^{-1})[59] and MeO (2033 cm^{-1}).[60]

The energy of the resolved A_1 stretch in the ^{MeO}TBDPhos complexes increased in the order of **8-MeOH** < **8** < **8-HNTf$_2$**,

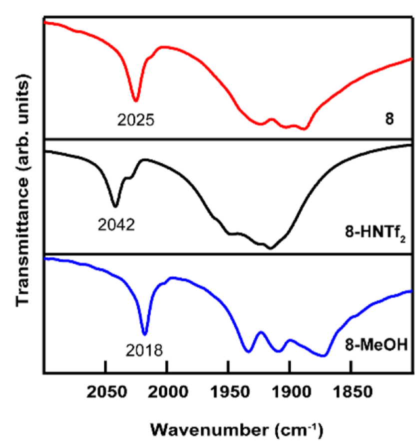

Figure 3. Infrared spectra (KBr) of Mo complexes **8**, **8-HNTf$_2$**, and **8-MeOH**.

https://dx.doi.org/10.1021/acs.organomet.0c00321
Organometallics 2020, 39, 2526−2533

and similar trends were observed for the less-resolved CO stretches provided in Table 3. The highest energy A_1 stretch in the borenium complex **8-HNTf$_2$** is attributed to decreased electron density and increased positive charge on the complex. This is consistent with changes expected based on a covalent bond perspective because the increased positive charge in **8-HNTf$_2$** should decrease M−CO π-backbonding. In contrast to **8-HNTf$_2$**, addition of MeOH to the more electron-deficient borane in **8** to form the four-coordinate borane in **8-MeOH** increases the electron density on the complex, thereby resulting in slightly more M−CO π-backbonding. While the covalent backbonding model provides an explanation consistent with our experimental observations, it is possible that the differences in CO stretching energies are due to electrostatic-induced changes in M−CO bond polarization.[61] Both explanations are plausible, and we cannot distinguish between the two given the data at hand.

DFT Calculations. DFT calculations were performed, using the Gaussian16 program,[62] to further evaluate the steric and electronic influence of phosphorus substituents on the reactivity of (TBDPhos)Pt($S_2C_6H_4$) complexes toward MeOH (eq 1). Geometry optimizations were performed using the M06-L density functional and the def2-SVP basis set for main group elements while the def2-TZVP and its corresponding ECP were used for Pt.[63,64] The nature of all stationary points were verified by harmonic vibrational analysis. Calculations were performed at room temperature and dichloromethane was used as the solvent. We also tested the choice of the meta-GGA M06-L functional against the hybrid B3LYP functional.[65] For optimizations using B3LYP, the choice of basis set and ECP remain the same; however, a dispersion correction (Grimme's D3 correction with Becke−Johnson damping)[66] has been incorporated. In addition to the experimentally tested ligands, we have extended our calculations to include ^{R}TBDPhos complexes with R = Me and EtO, and the previously reported ^{iPr}TBDPhos ligand.[44]

$$(^{R}\text{TBDPhos})\text{Pt}(\text{S}_2\text{C}_6\text{H}_4) + \text{MeOH} \rightarrow (^{R}\text{TBDPhos-MeOH})\text{Pt}(\text{S}_2\text{C}_6\text{H}_4) \quad (1)$$

The results, which are summarized graphically in Figure 4 and tabulated in Tables S1 and S2 (SI), show identical trends in ΔG regardless of functional, albeit with differences in the absolute values. Complexes with alkoxy substituents MeO and EtO yield the most exergonic reactions, whereas those with alkyl substituents ^{i}Pr and Et yield the most endergonic reactions, consistent with their lack of reactivity. The most endergonic reaction was predicted to be with (^{iPr}TBDPhos)-Pt($S_2C_6H_4$), which is consistent with the lack of ligand-centered reactivity reported previously for (^{iPr}TBDPhos)$NiCl_2$ and (^{iPr}TBDPhos)$PdCl_2$.[44] The lack of reactivity experimentally observed for phenyl-substituted **4** with MeOH suggests that the M06-L calculations are in better agreement with experiment than the B3LYP calculations. The calculated energy when R = Ph was nearly thermoneutral with M06-L (−0.93 kcal/mol), whereas the value from B3LYP is significantly more exergonic at −4.01 kcal/mol.

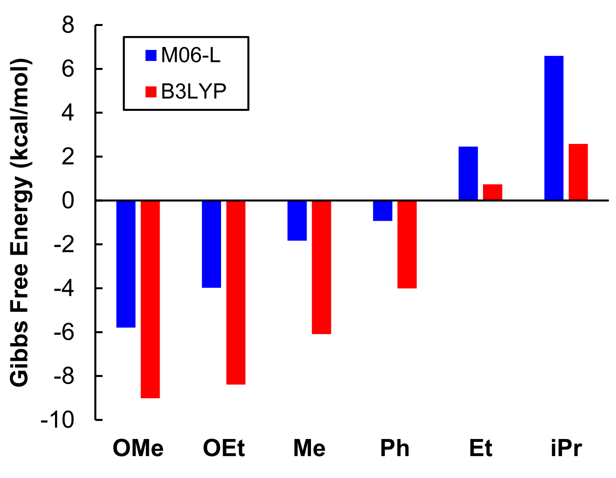

Figure 4. Comparison of Gibbs free energies computed using M06-L (blue bars) and B3LYP (red bars) functionals.

The DFT calculations corroborate the experimental results and show that both size and electronic properties of the substituents can have a pronounced influence on ligand-centered reactivity with MeOH. Side-by-side comparison of **5** and **6** show how electronic differences with similarly sized methoxy and ethyl substituents, respectively, significantly alter the ΔG of reaction. The electronic differences likely stem from the increased electron withdrawing properties of oxygen in the P−O bond that shifts electron density away from boron in the TBD backbone to form a more electrophilic borane. Indeed, Charge Model 5 (CM5)[67] calculations revealed the most positive charge on boron and nitrogen atoms on the TBD backbone when R = MeO or EtO (Table 4). However, the lack of a clear correlation between charge and ΔG for the other complexes, most notably when R = Me, suggests that the steric profile of the substituent must also be considered. Indeed, the expanded calculations show that increasing the length and size of the substituents causes the reaction to become more unfavorable regardless if the substituents are alkyl (Me < Et < ^{i}Pr) or alkoxy (MeO < EtO). Collectively, these data suggest that the most reactive TBDPhos ligands, at least from a thermodynamic perspective, are those with relatively small, electron-withdrawing substituents attached to phosphorus.

Table 4. Select CM5 Charges Calculated for (^{R}TBDPhos)Pt($S_2C_6H_4$)

R	Pt	B	N	N(P)	P
MeO	0.385	0.147	−0.307	−0.311	0.288
EtO	0.389	0.145	−0.308	−0.313	0.288
Ph	0.335	0.129	−0.308	−0.313	0.118
Me	0.317	0.133	−0.331	−0.317	0.109
Et	0.319	0.133	−0.315	−0.315	0.110
^{i}Pr	0.324	0.120	−0.313	−0.319	0.119

■ CONCLUSION

In summary, we have shown how phosphorus substituents can levy significant control over cooperative ligand-centered reactivity in TBDPhos complexes. Using MeOH as a test substrate for side-by-side comparisons, we showed that phenyl- and ethyl-substituted **4**, **6**, and **7** do not undergo ligand-centered reactions, whereas methoxy-substituted complexes **5** and **8** form **5-MeOH** and **8-MeOH** under identical conditions despite differences in ancillary ligands (dithiolate vs CO), metal identity (Pt vs Mo), and metal coordination geometry (square-planar vs octahedral).

Our results not only show how swapping phenyl and ethyl substituents for methoxy turns on ligand-centered reactivity in

https://dx.doi.org/10.1021/acs.organomet.0c00321
Organometallics 2020, 39, 2526−2533

the TBDPhos complexes studied here, they demonstrate how both steric and electronic modifications significantly removed from ligand reactive sites can be important considerations when designing chemically reactive ligands with Lewis acidic functional groups. In this context, these fundamental studies with an admittedly simple substrate (MeOH) have provided insights needed to make more informed decisions when testing TBDPhos complexes in different applications.

■ ASSOCIATED CONTENT

Supporting Information

The Supporting Information is available free of charge at https://pubs.acs.org/doi/10.1021/acs.organomet.0c00321.

Experimental details, tabulated crystallographic data, and NMR spectra (PDF)

XYZ coordinates of calculated structures (XYZ)

Accession Codes

CCDC 1958357−1958362 and 2001889 contain the supplementary crystallographic data for this paper. These data can be obtained free of charge via www.ccdc.cam.ac.uk/data_request/cif, or by emailing data_request@ccdc.cam.ac.uk, or by contacting The Cambridge Crystallographic Data Centre, 12 Union Road, Cambridge CB2 1EZ, UK; fax: +44 1223 336033.

■ AUTHOR INFORMATION

Corresponding Authors

Bess Vlaisavljevich − *Department of Chemistry, The University of South Dakota, Vermillion, South Dakota 57069, United States*; Email: bess.vlaisavljevich@usd.edu

Scott R. Daly − *Department of Chemistry, The University of Iowa, Iowa City, Iowa 52242, United States*; orcid.org/0000-0001-6229-0822; Email: scott-daly@uiowa.edu

Authors

Kyounghoon Lee − *Department of Chemistry, The University of Iowa, Iowa City, Iowa 52242, United States*

Johnathan D. Culpepper − *Department of Chemistry, The University of Iowa, Iowa City, Iowa 52242, United States*; orcid.org/0000-0002-7660-1641

Riffat Parveen − *Department of Chemistry, The University of South Dakota, Vermillion, South Dakota 57069, United States*

Dale C. Swenson − *Department of Chemistry, The University of Iowa, Iowa City, Iowa 52242, United States*

Complete contact information is available at: https://pubs.acs.org/10.1021/acs.organomet.0c00321

Notes

The authors declare no competing financial interest.

■ ACKNOWLEDGMENTS

This work was generously supported by the University of Iowa Center for Health Effects of Environmental Contamination (CHEEC), the American Chemical Society's Petroleum Research Fund (55989-DNI3), the National Science Foundation (CHE-1650894 and CHE-1828117), and National Science Foundation Graduate Research Fellowship Program NSF−GRFP under Grant No. (000390183) to JC. BV and RP thank the University of South Dakota for start-up funds. Computations supporting this project were performed on high performance computing systems at the University of South Dakota, funded by National Science Foundation Award 1626516. Any opinions, findings, and conclusions or recommendations expressed in this material are those of the authors and do not necessarily reflect views of the National Science Foundation.

■ REFERENCES

(1) Braunschweig, H.; Dewhurst, R. D.; Schneider, A. Electron-Precise Coordination Modes of Boron-Centered Ligands. *Chem. Rev.* **2010**, *110*, 3924−3957.

(2) Braunschweig, H.; Dewhurst, R. D. Transition Metals as Lewis Bases: "Z-type" Boron Ligands and Metal-to-Boron Dative Bonding. *Dalton Transactions* **2011**, *40*, 549−558.

(3) Amgoune, A.; Bourissou, D. σ-Acceptor, Z-type ligands for transition metals. *Chem. Commun.* **2011**, *47*, 859−871.

(4) Owen, G. R. Hydrogen Atom Storage upon Z-class Borane Ligand Functions: An Alternative Approach to Ligand Cooperation. *Chem. Soc. Rev.* **2012**, *41*, 3535−3546.

(5) Kameo, H.; Nakazawa, H. Recent Developments in the Coordination Chemistry of Multidentate Ligands Featuring a Boron Moiety. *Chem. - Asian J.* **2013**, *8*, 1720−1734.

(6) Spokoyny, A. M. New ligand platforms featuring boron-rich clusters as organomimetic substituents. *Pure Appl. Chem.* **2013**, *85*, 903−919.

(7) Devillard, M.; Bouhadir, G.; Bourissou, D. Cooperation between Transition Metals and Lewis Acids: A Way to Activate H_2 and H-E bonds. *Angew. Chem., Int. Ed.* **2015**, *54*, 730−732.

(8) Yamashita, M. The Organometallic Chemistry of Boron-Containing Pincer Ligands Based on Diazaboroles and Carboranes. *Bull. Chem. Soc. Jpn.* **2016**, *89*, 269−281.

(9) Owen, G. R. Functional Group Migrations Between Boron and Metal Centres within Transition Metal-Borane and -Boryl Complexes and Cleavage of H-H, E-H and E-E' Bonds. *Chem. Commun.* **2016**, *52*, 10712−10726.

(10) Maity, A.; Teets, T. S. Main Group Lewis Acid-Mediated Transformations of Transition-Metal Hydride Complexes. *Chem. Rev.* **2016**, *116*, 8873−8911.

(11) Li, Y.; Hou, C.; Jiang, J.; Zhang, Z.; Zhao, C.; Page, A. J.; Ke, Z. General H_2 Activation Modes for Lewis Acid-Transition Metal Bifunctional Catalysts. *ACS Catal.* **2016**, *6*, 1655−1662.

(12) Jones, J. S.; Gabbai, F. P. Coordination- and Redox-Noninnocent Behavior of Ambiphilic Ligands Containing Antimony. *Acc. Chem. Res.* **2016**, *49*, 857−867.

(13) Bouhadir, G.; Bourissou, D. Complexes of Ambiphilic Ligands: Reactivity and Catalytic Applications. *Chem. Soc. Rev.* **2016**, *45*, 1065−1079.

(14) Goettel, J. T.; Braunschweig, H. Recent advances in boron-centered ligands and their transition metal complexes. *Coord. Chem. Rev.* **2019**, *380*, 184−200.

(15) Pang, K.; Tanski, J. M.; Parkin, G. Reactivity of the Ni→B dative σ-bond in the Nickel Boratrane Compounds $[\kappa^4\text{-B}(\text{mim}^{\text{Bu}^t})_3]$-NiX (X = Cl, OAc, NCS, N_3): Synthesis of a Series of B-Functionalized Tris(2-mercapto-1-tert-butylimidazolyl)borato complexes, $[\text{YTm}^{\text{Bu}^t}]$NiZ. *Chem. Commun.* **2008**, 1008−1010.

(16) Tsoureas, N.; Kuo, Y.-Y.; Haddow, M. F.; Owen, G. R. Double Addition of H_2 to Transition Metal-Borane Complexes: a 'Hydride Shuttle' Process Between Boron and Transition Metal Centres. *Chem. Commun.* **2011**, *47*, 484−486.

(17) Harman, W. H.; Peters, J. C. Reversible H_2 Addition across a Nickel-Borane Unit as a Promising Strategy for Catalysis. *J. Am. Chem. Soc.* **2012**, *134*, 5080−5082.

(18) Kumar Podiyanachari, S.; Kehr, G.; Mueck-Lichtenfeld, C.; Daniliuc, C. G.; Erker, G. Remarkable Behavior of a Bifunctional Alkynylborane Zirconocene Complex toward Donor Ligands and Acetylenes. *J. Am. Chem. Soc.* **2013**, *135*, 17444−17456.

(19) Harman, W. H.; Lin, T.-P.; Peters, J. C. A d^{10} Ni-(H_2) Adduct as an Intermediate in H-H Oxidative Addition across a Ni-B Bond. *Angew. Chem., Int. Ed.* **2014**, *53*, 1081−1086.

(20) Cowie, B. E.; Emslie, D. J. H. Platinum Complexes of a Borane-Appended Analogue of 1,1'-Bis(diphenylphosphino)ferrocene: Flexi-

ble Borane Coordination Modes and in situ Vinylborane Formation. *Chem. - Eur. J.* **2014**, *20*, 16899−16912.

(21) Barnett, B. R.; Moore, C. E.; Rheingold, A. L.; Figueroa, J. S. Cooperative Transition Metal/Lewis Acid Bond-Activation Reactions by a Bidentate (Boryl)iminomethane Complex: A Significant Metal-Borane Interaction Promoted by a Small Bite-Angle LZ Chelate. *J. Am. Chem. Soc.* **2014**, *136*, 10262−10265.

(22) Figueroa, J. S.; Melnick, J. G.; Parkin, G. Reactivity of the Metal→BX_3 Dative σ-Bond: 1,2-Addition Reactions of the Fe→BX_3 Moiety of the Ferraboratrane Complex $[\kappa^4\text{-B}(\text{mim}^{\text{But}})_3]\text{Fe}(\text{CO})_2$. *Inorg. Chem.* **2006**, *45*, 7056−7058.

(23) Miller, A. J. M.; Labinger, J. A.; Bercaw, J. E. Homogeneous CO Hydrogenation: Dihydrogen Activation Involves a Frustrated Lewis Pair Instead of a Platinum Complex. *J. Am. Chem. Soc.* **2010**, *132*, 3301−3303.

(24) Miller, A. J. M.; Labinger, J. A.; Bercaw, J. E. Homogeneous CO Hydrogenation: Ligand Effects on the Lewis Acid-Assisted Reductive Coupling of Carbon Monoxide. *Organometallics* **2010**, *29*, 4499−4516.

(25) Miller, A. J. M.; Labinger, J. A.; Bercaw, J. E. Reductive Coupling of Carbon Monoxide in a Rhenium Carbonyl Complex with Pendant Lewis Acids. *J. Am. Chem. Soc.* **2008**, *130*, 11874−11875.

(26) Wade, C. R.; Gabbai, F. P. Cyanide Anion Binding by a Triarylborane at the Outer Rim of a Cyclometalated Ruthenium(II) Cationic Complex. *Inorg. Chem.* **2010**, *49*, 714−720.

(27) Jana, R.; Chakraborty, S.; Blacque, O.; Berke, H. Manganese and Rhenium Formyl Complexes of Diphosphinylborane Ligands: Stabilization of the Formyl Unit from Intramolecular B-O Bond Formation. *Eur. J. Inorg. Chem.* **2013**, *2013*, 4574−4584.

(28) Kiernicki, J. J.; Zeller, M.; Szymczak, N. K. Hydrazine Capture and N-N Bond Cleavage at Iron Enabled by Flexible Appended Lewis Acids. *J. Am. Chem. Soc.* **2017**, *139*, 18194−18197.

(29) Hale, L. V. A.; Szymczak, N. K. Hydrogen Transfer Catalysis beyond the Primary Coordination Sphere. *ACS Catal.* **2018**, *8*, 6446−6461.

(30) Kiernicki, J. J.; Norwine, E. E.; Zeller, M.; Szymczak, N. K. Tetrahedral iron featuring an appended Lewis acid: distinct pathways for the reduction of hydroxylamine and hydrazine. *Chem. Commun.* **2019**, *55*, 11896−11899.

(31) Kiernicki, J. J.; Shanahan, J. P.; Zeller, M.; Szymczak, N. K. Tuning ligand field strength with pendent Lewis acids: access to high spin iron hydrides. *Chemical Science* **2019**, *10*, 5539−5545.

(32) Kiernicki, J. J.; Zeller, M.; Szymczak, N. K. Requirements for Lewis Acid-Mediated Capture and N-N Bond Cleavage of Hydrazine at Iron. *Inorg. Chem.* **2019**, *58*, 1147−1154.

(33) Conifer, C. M.; Law, D. J.; Sunley, G. J.; White, A. J. P.; Britovsek, G. J. P. Lewis Acids and Lewis Acid-Functionalized Ligands in Rhodium-Catalyzed Methyl Acetate Carbonylation. *Organometallics* **2011**, *30*, 4060−4066.

(34) Fong, H.; Moret, M.-E.; Lee, Y.; Peters, J. C. Heterolytic H_2 Cleavage and Catalytic Hydrogenation by an Iron Metallaboratrane. *Organometallics* **2013**, *32*, 3053−3062.

(35) Lin, T.-P.; Peters, J. C. Boryl-Mediated Reversible H_2 Activation at Cobalt: Catalytic Hydrogenation, Dehydrogenation, and Transfer Hydrogenation. *J. Am. Chem. Soc.* **2013**, *135*, 15310−15313.

(36) Lin, T.-P.; Peters, J. C. Boryl-Metal Bonds Facilitate Cobalt/Nickel-Catalyzed Olefin Hydrogenation. *J. Am. Chem. Soc.* **2014**, *136*, 13672−13683.

(37) MacMillan, S. N.; Hill Harman, W.; Peters, J. C. Facile Si-H Bond Activation and Hydrosilylation Catalysis Mediated by a Nickel-Borane Complex. *Chemical Science* **2014**, *5*, 590−597.

(38) Inagaki, F.; Matsumoto, C.; Okada, Y.; Maruyama, N.; Mukai, C. Air-Stable Cationic Gold(I) Catalyst Featuring a Z-Type Ligand: Promoting Enyne Cyclizations. *Angew. Chem., Int. Ed.* **2015**, *54*, 818−822.

(39) Nesbit, M. A.; Suess, D. L. M.; Peters, J. C. E-H Bond Activations and Hydrosilylation Catalysis with Iron and Cobalt Metalloboranes. *Organometallics* **2015**, *34*, 4741−4752.

(40) Tseng, K.-N. T.; Kampf, J. W.; Szymczak, N. K. Modular Attachment of Appended Boron Lewis Acids to a Ruthenium Pincer Catalyst: Metal-Ligand Cooperativity Enables Selective Alkyne Hydrogenation. *J. Am. Chem. Soc.* **2016**, *138*, 10378−10381.

(41) Inagaki, F.; Nakazawa, K.; Maeda, K.; Koseki, T.; Mukai, C. Substituent effects in the cyclization of yne-diols catalyzed by gold complexes featuring L2/Z-type diphosphinoborane ligands. *Organometallics* **2017**, *36*, 3005−3008.

(42) Hirata, G.; Satomura, H.; Kumagae, H.; Shimizu, A.; Onodera, G.; Kimura, M. Direct Allylic Amination of Allylic Alcohol Catalyzed by Palladium Complex Bearing Phosphine-Borane Ligand. *Org. Lett.* **2017**, *19*, 6148−6151.

(43) Karunananda, M. K.; Mankad, N. P. Cooperative Strategies for Catalytic Hydrogenation of Unsaturated Hydrocarbons. *ACS Catal.* **2017**, *7*, 6110−6119.

(44) Lee, K.; Donahue, C. M.; Daly, S. R. Triaminoborane-Bridged Diphosphine Complexes with Ni and Pd: Coordination Chemistry, Structures, and Ligand-Centered Reactivity. *Dalton Transactions* **2017**, *46*, 9394−9406.

(45) Fritz, P.; Niedenzu, K.; Dawson, J. W. Boron-Nitrogen Compounds. XVII. Reactions of 1,8,10,9-Triazaboradecalin. *Inorg. Chem.* **1965**, *4*, 886−889.

(46) TBD is also a common acronym used to describe the structurally similar 1,5,7-triazabicyclo[4.4.0]dec-5-ene. This latter compound differs from 1,8,10,9-triazaboradecaline in that boron is replaced by an sp^2-hybridized carbon. In coordination chemistry, 1,5,7-triazabicyclo[4.4.0]dec-5-ene is often referred to by the acronym Hhpp (protonated form) or hpp (deprotonated form) instead of TBD, with hpp being derived from the alternative name hexahydropyrimidopyrimidine. We have encountered people that would prefer TBD in TBDPhos to mean 1,5,7-triazabicyclo[4.4.0]dec-5-ene instead of 1,8,10,9-triazaboradecaline, but we note that there appears to be only one report of a diphosphorus ligand derived from 1,5,7-triazabicyclo[4.4.0]dec-5-ene, and it was referred to as $(PPh_2)_2$-hpp consistent with the preferred use of hpp in coordination chemistry; see: Shang, C.; Vendier, L.; Sutra, P.; Igau, A. *Acta Crystallogr., Sect. E: Struct. Rep. Online* **2013**, *69*, m640−m641. We have found these discussions of our apparent commandeering of the TBD acronym to be quite amusing given that many phosphorus ligands have been named after the person or lab that discovered them instead of an acronym more relevant to their actual structure and composition. As such, we propose the alternative name "HoonPhos" after the person that initially discovered this class of ligands (and lead author of this paper) for those that hold strong reservations over our use of TBD.

(47) Lee, K.; Kirkvold, C.; Vlaisavljevich, B.; Daly, S. R. Ligand-Centered Borenium Reactivity in Triaminoborane-Bridged Diphosphine Complexes. *Inorg. Chem.* **2018**, *57*, 13188−13200.

(48) Lee, K.; Kim, C. W.; Buckley, J. L.; Vlaisavljevich, B.; Daly, S. R. Isolation of ligand-centered borocations in molybdenum complexes containing a triaminoborane-bridged diphosphorus ligand. *Dalton Transactions* **2019**, *48*, 3777−3785.

(49) Gutmann, V. Solvent Effects on the Reactivities of Organometallic Compounds. *Coord. Chem. Rev.* **1976**, *18*, 225−255.

(50) Beckett, M. A.; Strickland, G. C.; Holland, J. R.; Varma, K. S. A Convenient NMR Method for the Measurement of Lewis Acidity at Boron Centers: Correlation of Reaction Rates of Lewis Acid Initiated Epoxide Polymerizations with Lewis Acidity. *Polymer* **1996**, *37*, 4629−4631.

(51) Sivaev, I. B.; Bregadze, V. I. Lewis Acidity of Boron Compounds. *Coord. Chem. Rev.* **2014**, *270−271*, 75−88.

(52) Slawin, A. M. Z.; Wainwright, M.; Woollins, J. D. The preparation and coordination chemistry of phosphorus(III) derivatives of dialkyl ureas and thioureas. *J. Chem. Soc., Dalton Trans.* **2001**, 2724−2730.

(53) Nova, A.; Mas-Balleste, R.; Ujaque, G.; Gonzalez-Duarte, P.; Lledos, A. Aromatic C-F activation by complexes containing the $\{Pt_2S_2\}$ core via nucleophilic substitution: A combined experimental and theoretical study. *Dalton Transactions* **2009**, 5980−5988.

(54) Wrixon, J. D.; Hayward, J. J.; Raza, O.; Rawson, J. M. Oxidative addition chemistry of tetrathiocines: synthesis, structures and properties of group 10 dithiolate complexes. *Dalton Transactions* **2014**, *43*, 2134−2139.

(55) Waddell, P. G.; Slawin, A. M. Z.; Woollins, J. D. Correlating Pt-P bond lengths and Pt-P coupling constants. *Dalton Trans.* **2010**, *39*, 8620−8625.

(56) Piers, W. E.; Bourke, S. C.; Conroy, K. D. Borinium, Borenium, and Boronium Ions: Synthesis, Reactivity, and Applications. *Angew. Chem., Int. Ed.* **2005**, *44*, 5016−5036.

(57) De Vries, T. S.; Prokofjevs, A.; Vedejs, E. Cationic Tricoordinate Boron Intermediates: Borenium Chemistry from the Organic Perspective. *Chem. Rev.* **2012**, *112*, 4246−4282.

(58) Eisenberger, P.; Crudden, C. M. Borocation catalysis. *Dalton Transactions* **2017**, *46*, 4874−4887.

(59) Gaebelein, H.; Ellermann, J. Complex chemistry of polyfunctional ligands. XLIII. Vibration spectroscopic studies of tetracarbonylmetal derivatives of ditertiary phosphines. *J. Organomet. Chem.* **1978**, *156*, 389−402.

(60) King, R. B.; Rhee, W. M. Poly(tertiary phosphines and arsines). 16. Some metal carbonyl complexes of 1,2-bis(dimethoxyphosphino)-ethane. *Inorg. Chem.* **1978**, *17*, 2961−2963.

(61) Goldman, A. S.; Krogh-Jespersen, K. Why Do Cationic Carbon Monoxide Complexes Have High C-O Stretching Force Constants and Short C-O Bonds? Electrostatic Effects, Not σ-Bonding. *J. Am. Chem. Soc.* **1996**, *118*, 12159−12166.

(62) Frisch, M. J.; Trucks, G. W.; Schlegel, H. B.; Scuseria, G. E.; Robb, M. A.; Cheeseman, J. R.; Scalmani, G.; Barone, V.; Petersson, G. A.; Nakatsuji, H.; Li, X.; Caricato, M.; Marenich, A. V.; Bloino, J.; Janesko, B. G.; Gomperts, R.; Mennucci, B.; Hratchian, H. P.; Ortiz, J. V.; Izmaylov, A. F.; Sonnenberg, J. L.; Williams-Young, D.; Ding, F.; Lipparini, F.; Egidi, F.; Goings, J.; Peng, B.; Petrone, A.; Henderson, T.; Ranasinghe, D.; Zakrzewski, V. G.; Gao, J.; Rega, N.; Zheng, G.; Liang, W.; Hada, M.; Ehara, M.; Toyota, K.; Fukuda, R.; Hasegawa, J.; Ishida, M.; Nakajima, T.; Hon-da, Y.; Kitao, O.; Nakai, H.; Vreven, T.; Throssell, K.; Montgomery, J. A., Jr.; Peralta, J. E.; Ogliaro, F.; Bearpark, M. J.; Heyd, J. J.; Brothers, E. N.; Kudin, K. N.; Staroverov, V. N.; Keith, T. A.; Kobayashi, R.; Normand, J.; Raghavachari, K.; Rendell, A. P.; Burant, J. C.; Iyengar, S. S.; Tomasi, J.; Cossi, M.; Millam, J. M.; Klene, M.; Adamo, C.; Cammi, R.; Ochterski, J. W.; Martin, R. L.; Morokuma, K.; Farkas, O.; Foresman, J. B.; Fox, D. J. *Gaussian 16*, rev. A.03; Gaussian, Inc.: Wallingford, CT, 2016.

(63) Weigend, F.; Ahlrichs, R. Balanced basis sets of split valence, triple zeta valence and quadruple zeta valence quality for H to Rn: Design and assessment of accuracy. *Phys. Chem. Chem. Phys.* **2005**, *7*, 3297−3305.

(64) Zhao, Y.; Truhlar, D. G. A new local density functional for main-group thermochemistry, transition metal bonding, thermochemical kinetics, and noncovalent interactions. *J. Chem. Phys.* **2006**, *125*, 194101.

(65) Becke, A. D. A new mixing of Hartree-Fock and local-density-functional theories. *J. Chem. Phys.* **1993**, *98*, 1372−1377.

(66) Grimme, S.; Antony, J.; Ehrlich, S.; Krieg, H. A consistent and accurate ab initio parametrization of density functional dispersion correction (DFT-D) for the 94 elements H-Pu. *J. Chem. Phys.* **2010**, *132*, 154104.

(67) Marenich, A. V.; Jerome, S. V.; Cramer, C. J.; Truhlar, D. G. Charge Model 5: An Extension of Hirshfeld Population Analysis for the Accurate Description of Molecular Interactions in Gaseous and Condensed Phases. *J. Chem. Theory Comput.* **2012**, *8*, 527−541.

https://dx.doi.org/10.1021/acs.organomet.0c00321
Organometallics 2020, 39, 2526−2533